

Chaos control in solar fed DC-DC boost converter by optimal parameters using nelder- mead algorithm powered enhanced BFOA

Sudhakar N, Rajasekar N, Saya Akhil and Jyotheeswara Reddy K

School of Electrical Engineering, VIT University, Vellore-632014, Tamil Nadu, India.

Email: nsudhakar@vit.ac.in

Abstract: The boost converter is the most desirable DC-DC power converter for renewable energy applications for its favorable continuous input current characteristics. In other hand, these DC-DC converters known as practical nonlinear systems are prone to several types of nonlinear phenomena including bifurcation, quasiperiodicity, intermittency and chaos. These undesirable effects has to be controlled for maintaining normal periodic operation of the converter and to ensure the stability. This paper presents an effective solution to control the chaos in solar fed DC-DC boost converter since the converter experiences wide range of input power variation which leads to chaotic phenomena. Controlling of chaos is significantly achieved using optimal circuit parameters obtained through Nelder-Mead Enhanced Bacterial Foraging Optimization Algorithm. The optimization renders the suitable parameters in minimum computational time. The results are compared with the traditional methods. The obtained results of the proposed system ensures the operation of the converter within the controllable region.

1. Introduction

The role of solar energy in distributed power generation system has become inevitable in order to meet out the increasing power demands. With no pollutant emission, Photovoltaic cells convert sunlight directly to electricity. However, the generated voltage, current and power are unceasingly varying depends on the incident of solar energy and most of the time the voltage produced by the PV module is inadequate due to various parameters. Hence the DC-DC boost converter as an intermediate power processing unit plays very vital role in between the solar panel and load [1].

Power converters are usually designed to function in a stable manner in its normal operating region. Outside of these conditions the converter can experience period doubling bifurcations (forking) that can develop into chaos (unpredictability). DC-DC boost converter experiences such nonlinear operating conditions when connected to the solar panel whose output varies very often with respect to the



irradiation and temperature. Generally, whenever the chaotic behavior occurs, it can cause additional losses, noise, ripples, other unwanted outputs and even leads to catastrophic failure of the converter. Instability, spurious oscillations and sub harmonics have been exclusively observed in fast switching power converters when they fail to maintain their normal periodic operation. Hence, chaos should be reduced as much as possible, or totally eliminated [2].

Under certain parametric conditions, due to its inherent non-linearity the DC–DC converter emerges some collapse of operating mode, EMI and functioning out of order after long running. As the small change or interruption in the system dynamics leads to these above said undesirable complicated chaotic behaviors, selection of system parameter value has to be given with much importance, failing which will greatly limits the DC–DC converter applications. Out of so many parameters of converter, the Resistor (R), Inductor (L) and Capacitor (C) are accounted for optimization since they greatly involved in determining the converter dynamics [3].

Many methods have been proposed for controlling of chaos in nonlinear systems. However, the chaos control methods can be broadly classified into Parametric Variation Methods (method of OGY), Controlling via External Force, Entrainment and Migration Controls, Engineering Control Approaches such as Intelligent Control, Neural Network approach, Synchronization of Chaos, Introduction of a controller (classical PI, PID, linear or nonlinear, stochastic etc.,).

In this proposed work, the controlling of chaos is achieved by optimized system parameters. The optimization is carried out by very familiar bio-inspired Bacterial Foraging Optimization Algorithm enhanced with Nelder-Mead algorithm for computing the optimal parameters in trivial duration [4]. The bifurcation analysis substantiates the effective controlling of chaos in voltage mode controlled DC-DC boost converter with enhanced BFA and the results are compared with the traditional methods. The convergence process of different optimization techniques is also analyzed. The general block diagram of the proposed work is shown in Figure.1.

The organization of the paper is as follows, the second section discusses importance of PV cell and its modeling. The third section explains the closed loop operation of the boost converter and the necessity of optimizing the resistor, inductor and the capacitor. The enhanced BFA algorithm is discussed in section 4. The results of the boost converter with unoptimized values are given in section 5 and is followed by the results of the boost converter with optimized values and its bifurcation analysis in section 6. Bifurcation behavior of boost converter for different operating region is summarized in section 7.

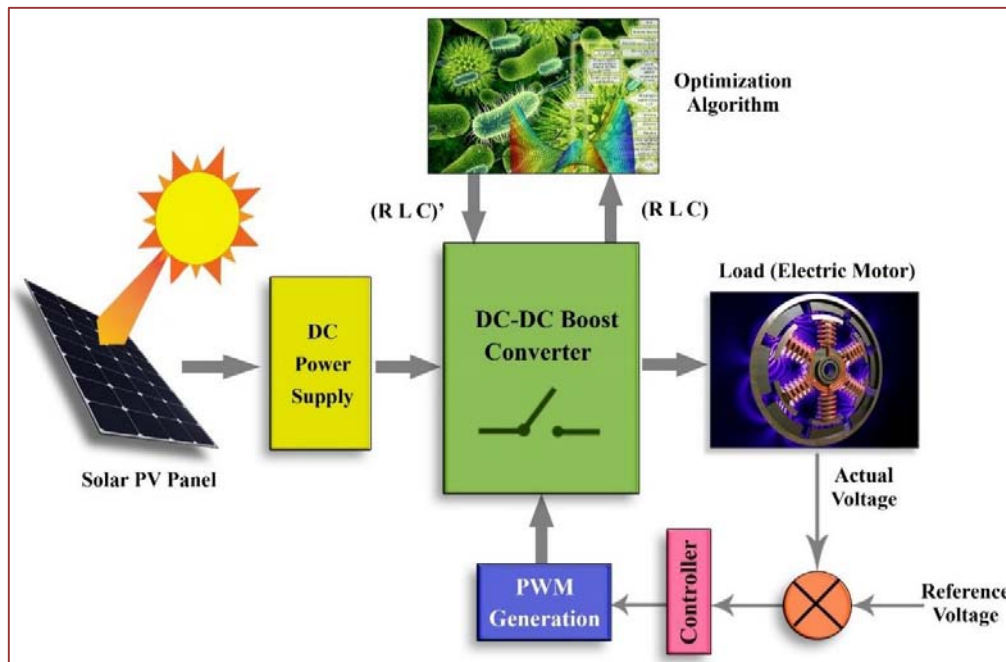


Figure 1. General Block diagram of voltage mode controlled boost converter with optimized parameters

2. Photo voltaic cell model

The photo voltaic source is basically a current source, whose value is dependent on the incident solar radiation. The whole cell acts like a P-N junction diode. When solar radiation incident on PV cell it creates electron-hole pairs, are separated by PN junction. Electrons move toward N-side and holes move toward P-side which causes the flow of current called photo current. Flow of electrons and holes are resisted by resistance in their path called series resistance R_s which will be in series in the circuit. These electrons holes pairs collected by electrodes. Some of the electrons and holes recombine before reaching the electrodes. This is called shunting effect and so the equivalent resistance R_{sh} in parallel in the circuit [5]. The equivalent circuit is shown in Figure.2.

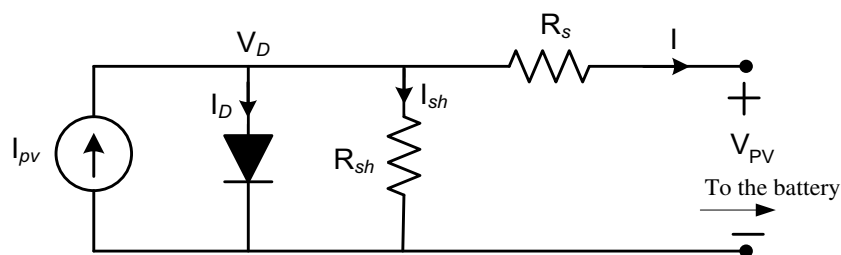


Figure 2. Equivalent circuit of a PV cell

Diode current is given by:

$$I_D = I_s \left(\exp^{\frac{q(V_{PV} + R_s I)}{NKT}} - 1 \right) \quad (1)$$

Applying KCL equation to the equivalent circuit model shown in Figure.2

$$I_{pv} - I_D - I_{sh} - I = 0 \quad (2)$$

$$I_{sh} = \frac{V_D}{R} \quad \text{And} \quad V_D = V_{PV} + R_s I \quad (3)$$

Current to the load is given by

$$I = I_{pv} - I_s \left(\exp^{\frac{q(V_{PV} + R_s I)}{NKT}} - 1 \right) - \frac{(V_{PV} + R_s I)}{R_{sh}} \quad (4)$$

In the above equation, I_{pv} is the photocurrent, I_s is the reverse saturation current of the diode, q is the electron charge, V is the voltage across the diode, K is the Boltzmann's constant, T is the junction temperature, N is the ideality factor of the diode, and R_s and R_{sh} are the series and shunt resistors of the cell, respectively. So, a PV cell's physical behavior can be described in term of I_{pv} , I_s , R_s , R_{sh} and it completely depends on two environmental factors i.e. temperature and solar radiation. Photo current (I_{pv}) is given by equation (5).

$$I_{ph} = [I_{sc} + k_i(T - 298)] \frac{\beta}{1000} \quad (5)$$

K_i is the cell's short circuit current temperature coefficient (A/C)

β is the solar radiation (W/m^2).

3. Voltage mode controlled boost converter

The power produced by the PV panel has to be processed before delivering to the load, and the boost converter is a basic DC-DC converter that is often satisfies this purpose. The boost converter is basically an electronic circuit where the output voltage is greater than the input voltage. The regulation of voltage across the load is assured by varying the PWM switching pulse at fixed frequency. The PWM pulse is varied by voltage controlled feedback path designed for the operation of variable range of output voltage. The circuit diagram for the proposed scheme is shown in Figure.3 where, the DC-DC boost converter fed by PV Module, Diode (D), Switch (S), inductor (L), capacitor (C) and load resistor (R) belongs to the power circuit [6]. The design equations are as follows,

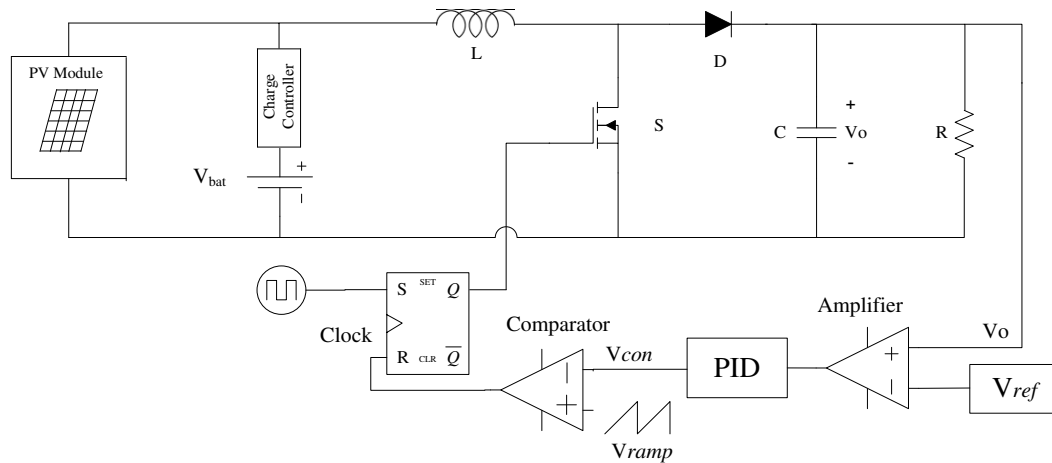


Figure 3. Closed Loop Control of Boost Converter

$$L_{\min} = \frac{D(1-D)^2 R}{2f_s} \quad (6)$$

$$I_L = \frac{V_{in}}{(1-D)^2 R} \quad (7)$$

$$C \geq \frac{D}{R(\Delta V_o/V)f_s} \quad (8)$$

Assuming the circuit to be in continuous conduction mode, it can be divided into two modes: (a) When the switch (S) is turned ON, the inductor current rises and energy is stored in it and (b) When the switch (S) is turned OFF, the stored energy is delivered to the load. The inductor current falls, and the voltage across it adds up to the applied voltage V_{in} and appears across the load.

When the switch S is turned ON, the state equations are:

$$\frac{V_L}{L} = \frac{di_L}{dt} \quad (9)$$

$$\frac{dV_o}{dt} = -\frac{V_o}{RC} \quad (10)$$

When the switch S is turned OFF, the state equations are

$$\frac{di_L}{dt} = \frac{V_L - V_o}{L} \quad (11)$$

When the converter is connected to the PV panel, the input voltage is not constant, and depends on the instantaneous values of the current and consequently the output voltage also. To achieve a constant output voltage, duty cycle of boost converter is controlled by using voltage mode control. The output voltage to controlling duty cycle transfer function of the DC-DC converter is given as:

$$\frac{V_o(S)}{d(S)} = \frac{(1-D)V_o + (LI_L)S}{LCS^2 + (L/R)S + (1-D)^2} \quad (12)$$

The controller's transfer function is given as:

$$G_c(S) = K_p (1 + 1/T_i S + T_d S) \quad (13)$$

Where,

K_p - proportionality constant of the controller

T_i -Integral tuning constant of the controller

T_d -Derivative tuning constant of the controller

By using the values from the equations (12)-(13), the PID controller [7] is tuned so to obtain the control voltage which is the difference between the constant reference voltage and the output voltage.

$$V_{con} = K_p (V_o - V_{ref}) + K_i \int (V_o - V_{ref}) dt + K_d (V_o - V_{ref}) / dt \quad (14)$$

This control voltage is then compared with ramp voltage which is given by equation (14). Output from comparator is then given at RESET pin of SR flip flop and clock pulse is given to SET pin of flip flop [8]. At the start of each clock cycle, the switch is ON. When $V_{con} = V_{ramp}$, the switch is OFF for the rest of the cycle.

$$V_{ramp} = V_U - V_L \frac{t}{T} \bmod 1 \quad (15)$$

4. The enhanced bacterial foraging algorithm

Bacterial Foraging Algorithm (BFA), proposed by Passino belongs to the nature-inspired optimized algorithm's family [9-11]. BFA has been successfully applied to variety of engineering problems, such as PID controller, harmonic estimation, transmission loss reduction, antenna parameter calculation, image demonizing, economic load dispatch and machine learning etc., BFA contains population of bacteria which is group of potential solutions for design of boost converter. Each bacteria gives solution in terms of values resistor, inductor and capacitor. BFA mimics the four principal mechanisms observed in a real bacterial system: chemo taxis, swarming, reproduction, and elimination-dispersal to solve this non-gradient optimization problem. In Chemotaxis process Bacteria follows path to reach toward nutrients gradient and avoid toxic environment. A fitness value is assigned to each bacteria according to fitness function which has to be maximized for the optimization problem. Steps involved in optimization technique are as follows:

4.1. Initialization

Bacteria size (b), the number of chemotactic steps (N_c), the swimming length (N_s), the number of reproduction steps (N_{re}), the number of elimination-dispersal events (N_{ed}), Elimination-dispersal probability (P_{ed}), dimension search space (p). All bacteria are initialized will lie within the design limits.

4.2. Chemotaxis

During chemo taxis, the bacteria climb the nutrient concentration, avoid noxious substances, and search for a way out of the neutral media. This process is achieved through swimming and tumbling. Bacterial chemo taxis is a complex combination of swimming and tumbling that keeps bacteria in places of higher concentration of nutrients. Bacterial chemo taxis can also be considered as the optimization process of the exploitation.

4.3. Nelder- Mead Algorithm

For further enhancing the BFA, a simplex algorithm called Nelder Mead is added to the optimization technique to find local minimum of function of several variables. We use the Nelder–Mead method based on the comparison of the function values at the $n + 1$ vertices for n -dimensional decision variables to solve our optimization problem. The calculation at each time will generate a new vertex for the simplex. If this new point is better than at least one of the existing vertices, it replaces the worst vertex. The simplex vertices are changed through reflection, expansion, shrinkage and contraction operations in order to find an improving solution. For two variables, a simplex is a triangle, and the method is a pattern search that compares function values at the three vertices of a triangle. The process generates a sequence of triangles (which might have different shapes), for which the function values at the vertices become smaller and smaller. The size of the triangle is reduced and the coordinates of the minimum point are found. The values obtained after the chemotactic process are put to this process before reproduction to obtain best bacteria. The Nelder-Mead algorithm is implemented after Chemotaxis process. The same is shown in Figure 3. as a shaded box to distinguish from the conventional BFA and updates the value.

4.4. Reproduction

During reproduction, all bacteria are sorted in reverse order according to fitness values. The least healthy bacteria (those yielding lower value of the objective function) die and the rest healthiest bacteria each splits into two bacteria, which are placed in the same. This makes the population of bacteria remains constant. The reproduction process of bacterial foraging aims to speed up the convergence suitable in static problems, but not in dynamic environment.

4.5. Elimination and Dispersal

Gradual or sudden changes in the local environment where a bacterium population lives may occur due to various reasons e.g. a significant local rise of temperature may kill a group of bacteria that are currently in a region with a high concentration of nutrient gradients. Events can take place in such a fashion that all the bacteria in a region are killed or a group is dispersed into a new location. To simulate this phenomenon in EBFA some bacteria are liquidated at random with a very small probability while the new replacements are randomly initialized over the search space. Elimination and dispersal helps to avoid premature convergence or, being trapped in local optima. The flow chart is shown in Figure.3.

The enhanced BFA technique is applied to optimize the design parameters of the DC-DC boost converter. The bacterial structure is represented in terms of inductor, capacitor and resistor.

Bacterial structure = [R L C]

Each parameter is restricted to be within the specified range of design consideration. The Fitness function [12] representing the stability of the process and its response is given by:

$$\text{Minimize } fitnessfunc = \sum [|e_j| + |\Delta e_j|] \quad (16)$$

Where,

e_j is the error between output voltage and reference voltage.

Δe_j is the error correction at instant j .

The parameters used for executing the enhanced BFA technique are:

- No. of bacteria – 50
- Chemotactic step size (N_c) – 4
- Reproduction Loop size (N_{re}) – 4

- Elimination and dispersal loop size (N_{ed}) – 2
- Maximum no of swim length (N_s) – 4
- Dispersal Probability (P_{ed}) – 0.2

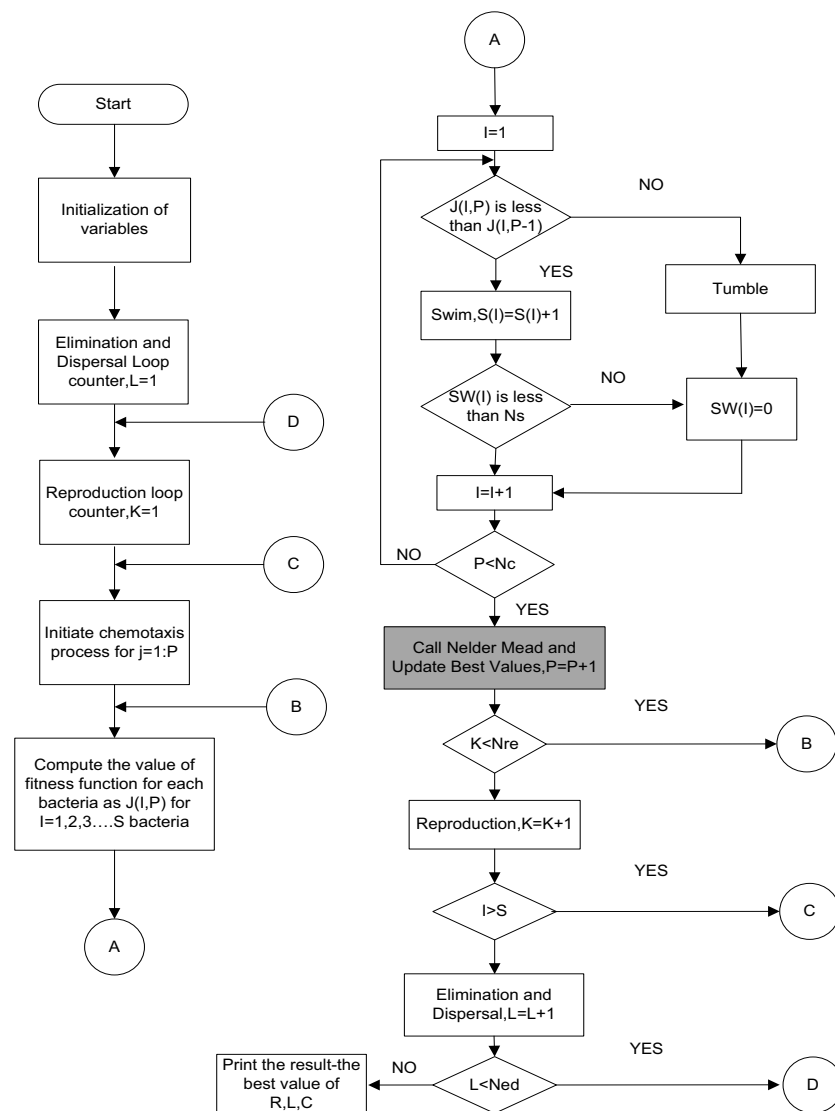
The algorithm is implemented using MATLAB Script. The code monitors the fitness function and the corresponding bacteria value is considered.

5. Analysis With Unoptimized Parameters

The specifications of the WS-10 solar panel and the circuit parameters are shown in Table 1. The system is simulated in MATLAB/SIMULINK and the solver opted is 'ode15s'. The simulation diagram is shown in Figure.5. The P-V and I-V characteristics of the PV module is shown for different irradiances in Figure.6 (a) and Figure.6 (b). The maximum power point is obtained at a voltage of 17.3V. From Figure.6 (a) and Figure.6 (b), it is observed that the power and the current requirement of the DC-DC boost converter for irradiation values of 1000 W/m^2 , 800 W/m^2 and 600 W/m^2 . For a condition where the irradiation value is less than 400 W/m^2 , the PV module is not capable to meet the converter's power requirement. The output voltage, inductor current waveforms and their phase portrait (x-axis – inductor current in Ampere, y-axis – output voltage in Volts) at different values of $V_{in} = 12, 16$ and 20V is shown in Figure.7, Figure. 8 and Figure.9 respectively for the designed values. The input voltages are so chosen to show different periods of operation in a DC-DC boost converter.

Table 1. Circuit Parameters and specification of WE-10 Solar Panel

<i>Circuit specifications</i>		<i>Solar Panel Specifications</i>	
Input Voltage (V_{in})	12V-22V	Maximum Power	10 W
Output Voltage(V_o)	24 V	Voltage at Pmax	17 V
Resistor (R)	100 Ω	Current at Pmax	0.68 A
Inductor(L)	625 μH	Open circuit Voltage ($V_{o.c}$)	22 V
Capacitor	5 μH	Short Circuit Current ($I_{s.c}$)	0.65 A
Switching Frequency (f_s)	100 kHz		

**Figure 4.** Nelder algorithm

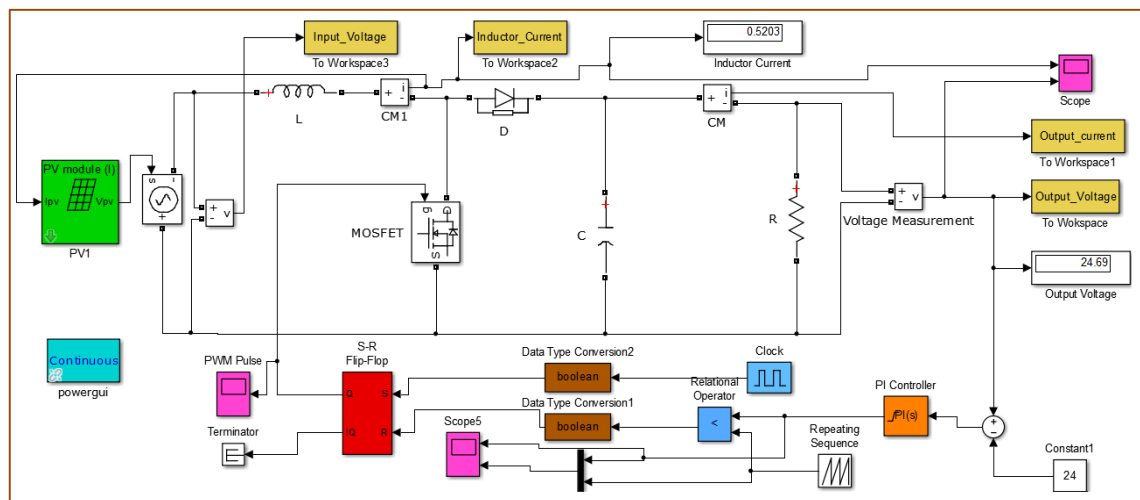
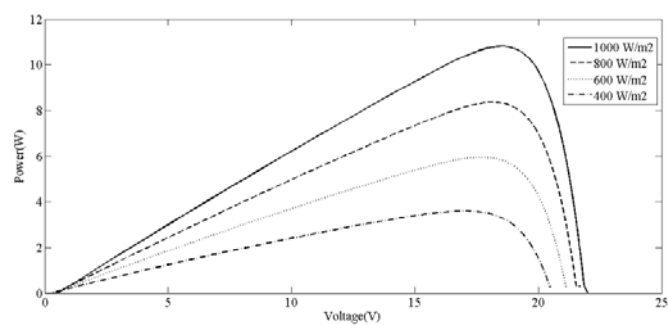
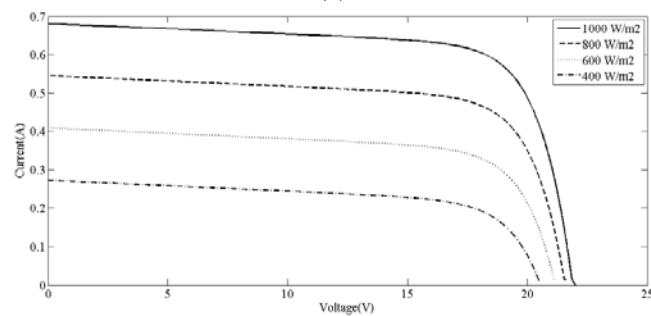


Figure 5. Simulink diagram of solar PV fed closed loop DC-DC boost converter

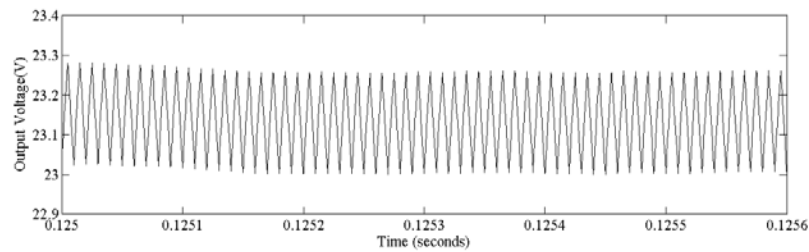


(a)

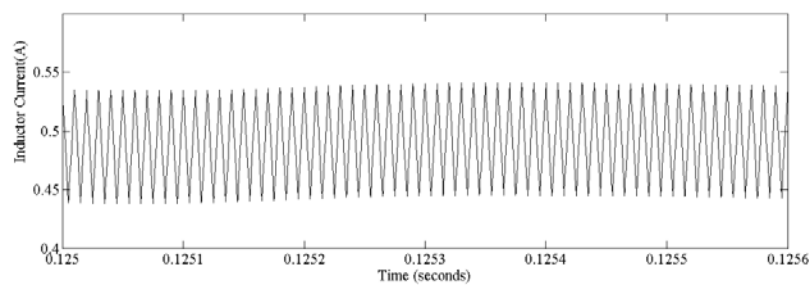


(b)

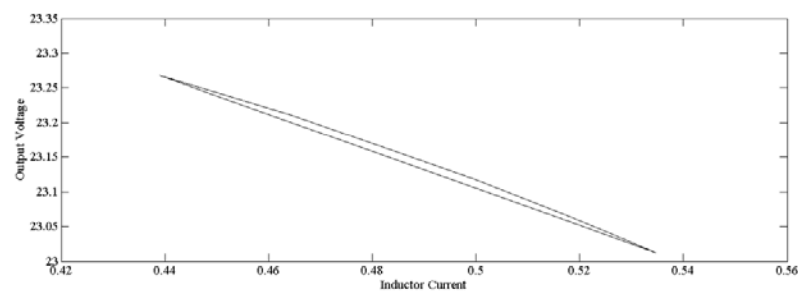
Figure 6. (a) P-V characteristics of photovoltaic module (b) I-V characteristics photovoltaic module



(a)

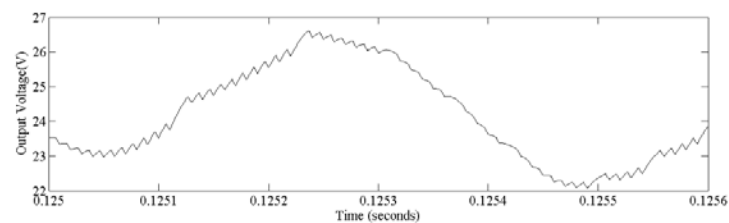


(b)



(c)

Figure 7. (a) Output voltage waveform (b) Inductor current waveform (c) Phase portrait for Period 1 operation of boost converter with unoptimized parameters at $V_{in}=12V$



(a)

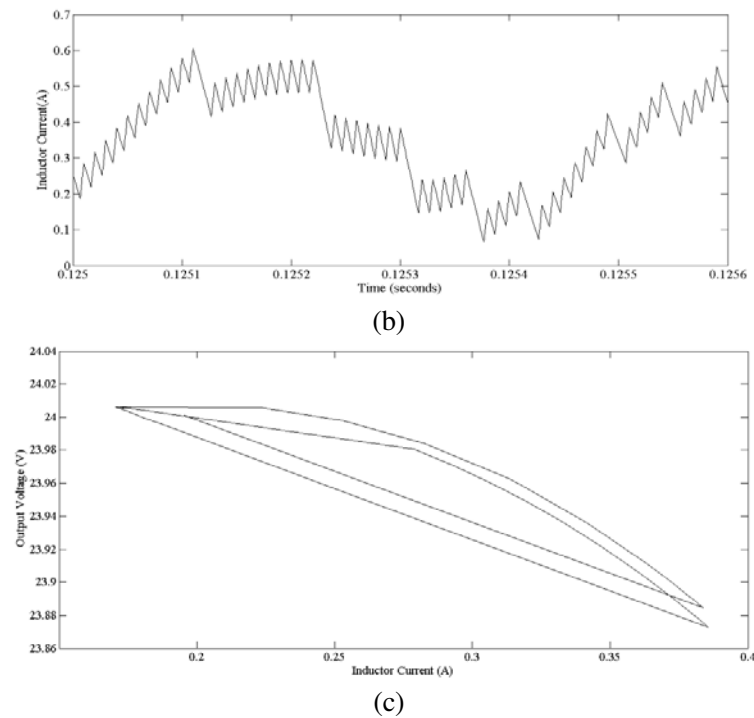
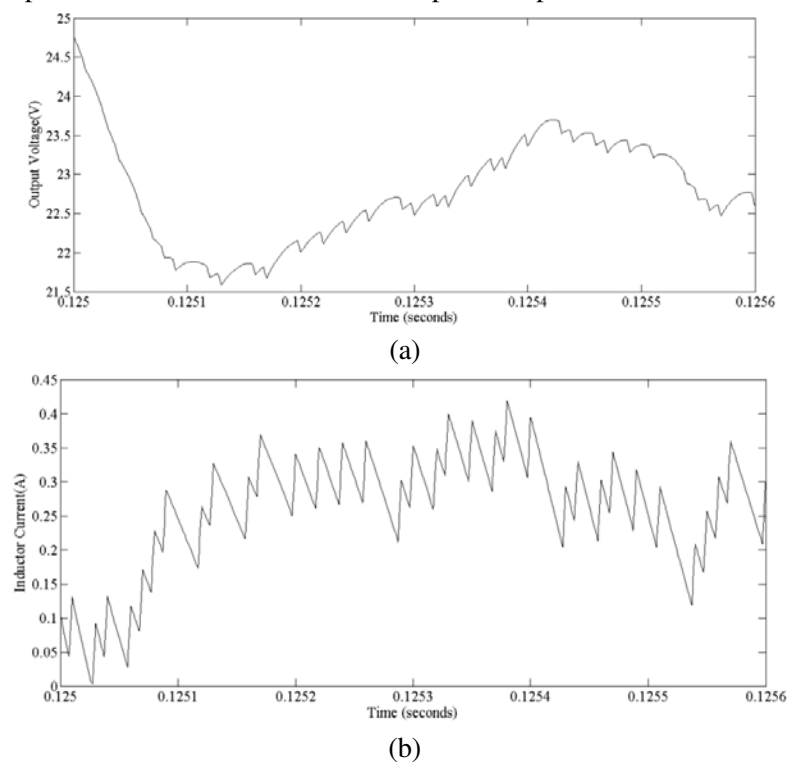


Figure 8. (a) Output voltage waveform (b) Inductor current waveform (c) Phase portrait for Period 2 operation of boost converter with unoptimized parameters at $V_{in}=16V$



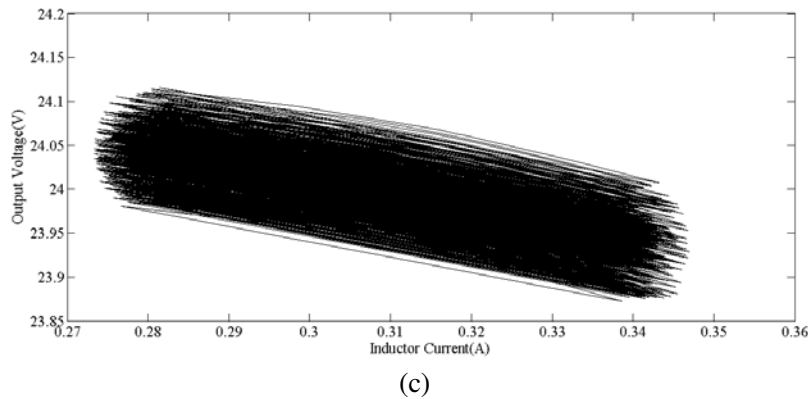


Figure 9.(a)Outputvoltage waveform (b) Inductor current waveform (c) Phase portrait for Chaos operation of boost converter with unoptimized parameters at $V_{in} = 20V$

6. Analysis with Optimized parameters

The Figure. 10, Figure. 11, Figure. 12, Figure.13, Figure.14, Figure.15 shows the output voltage, inductor current and the phase portrait for $V_{in} = 12V$, $16V$ and $20V$ for the optimized parameters using BFA and EBFA respectively. The designed values of R , L , and C for the given rating of boost converter and the optimized values by different techniques are listed out in Table 2.

Table 2. Circuit Parameters obtained by different techniques

<i>Parameter</i>	<i>By design</i>	BFA	EBFA
Inductor L (Henry)	6.25e-4	2.3e-4	2.84e-4
Capacitance C (Farad)	5e-6	4.78e-6	3.6e-6
Resistance R (Ohm)	100	125.6	110.2

For $V_{in}=12V$, It is observed that the phase portrait for parameters by design is better than for the optimized values. But for other cases of $V_{in}=16V$ and $20V$, the system dynamics are considerably disturbed. The system dynamics at $V_{in} = 12V$ can be compromised for optimization parameters as it is still very much under the limit. The phase portraits can be particularly compared for different V_{in} values as it clearly states that the scrolls are being reduced after optimizing the system parameters. It can also be observed that the system parameters obtained by EBFA are more effective than those of BFA and the results obtained are also supports the EBFA as shown in Figure.11(c), Figure.12(c) and Figure.14(c), Figure.15(c) Respectively.

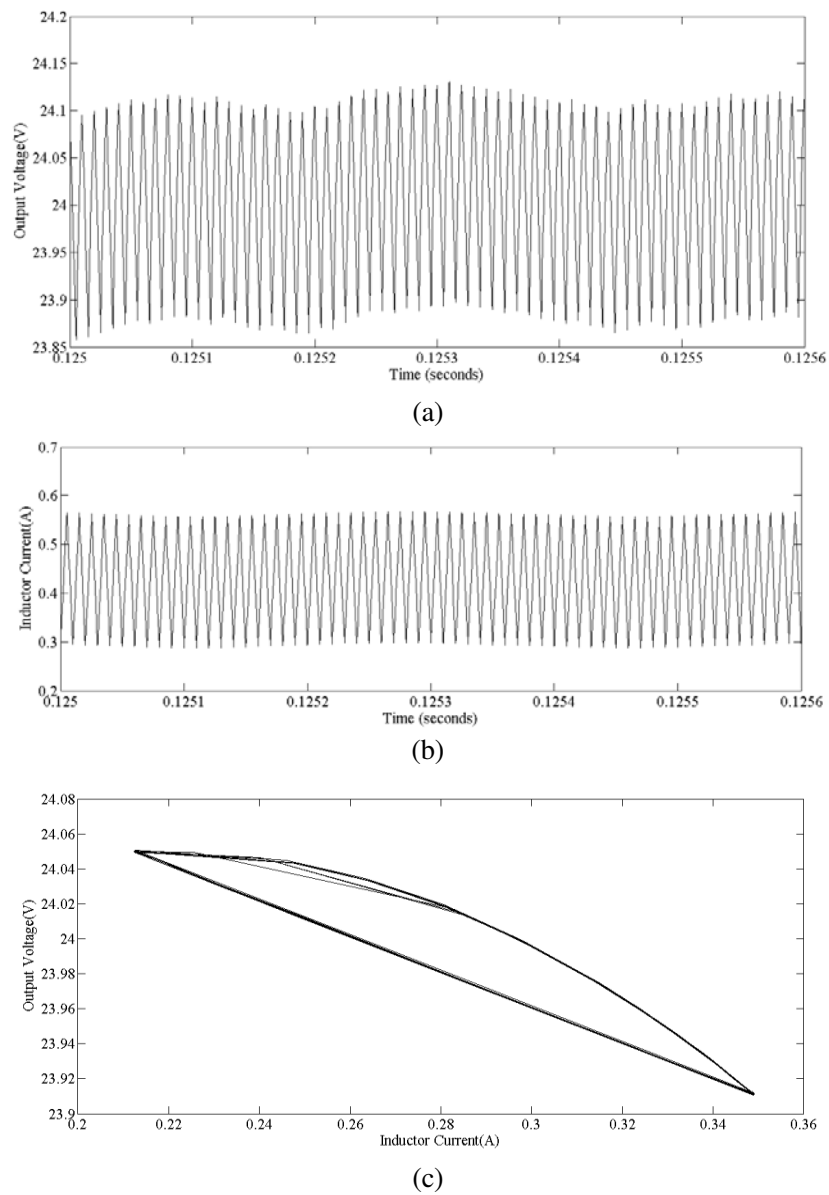


Figure 10. (a) Outputvoltage waveform (b) Inductor current waveform (c) Phase portrait for Period 1 operation of boost converter after optimization using BFA at $V_{in} = 12$ V

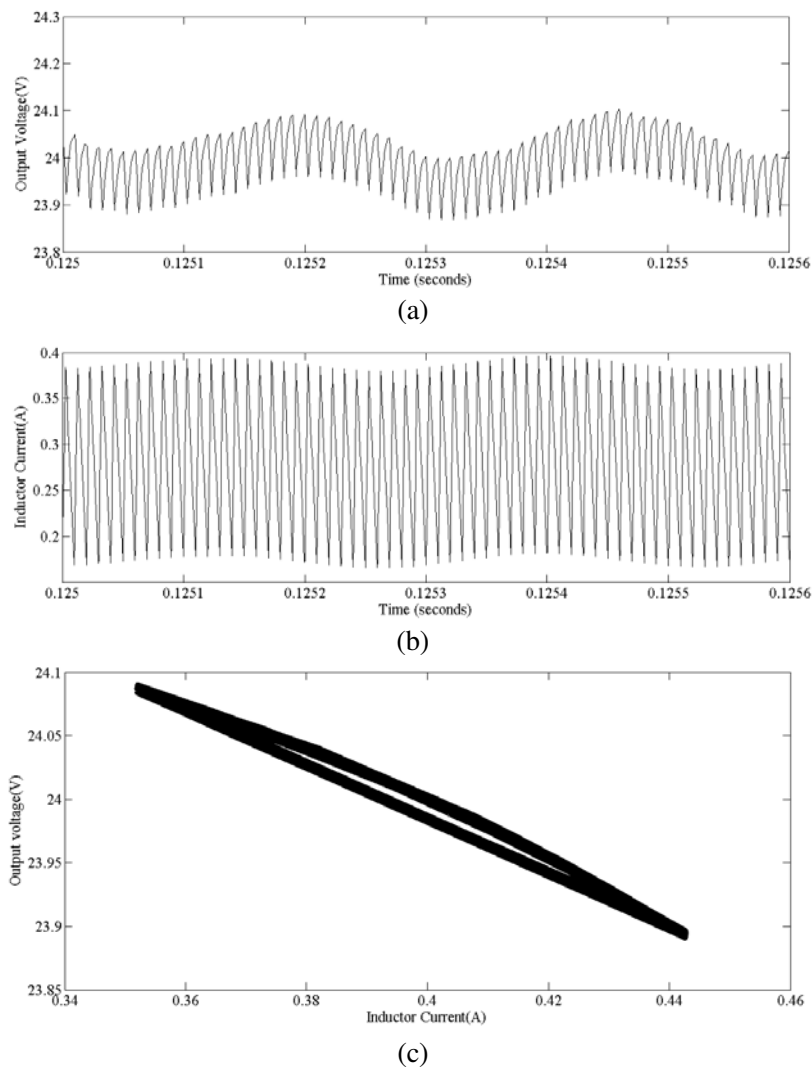
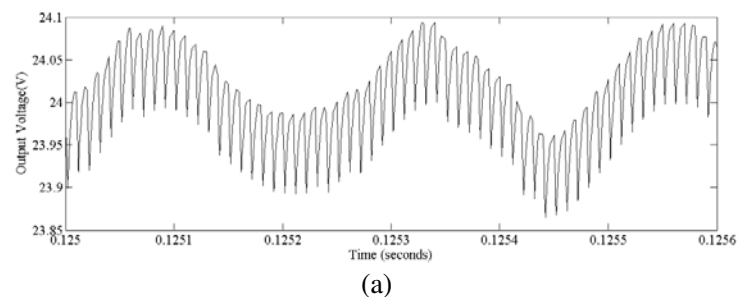


Figure 11. (a) Output voltage waveform (b) Inductor current waveform (c) Phase portrait for Period 1 operation of boost converter after optimization using BFA at $V_{in}=16V$



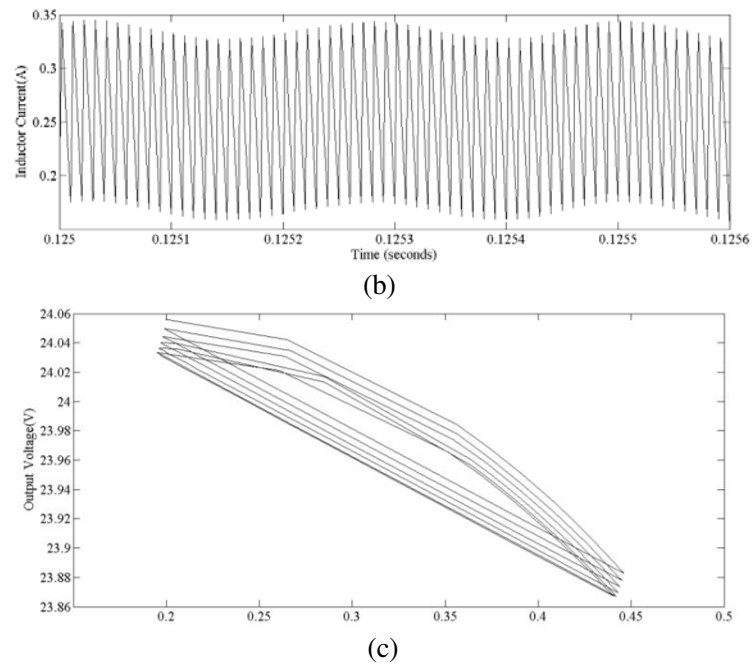
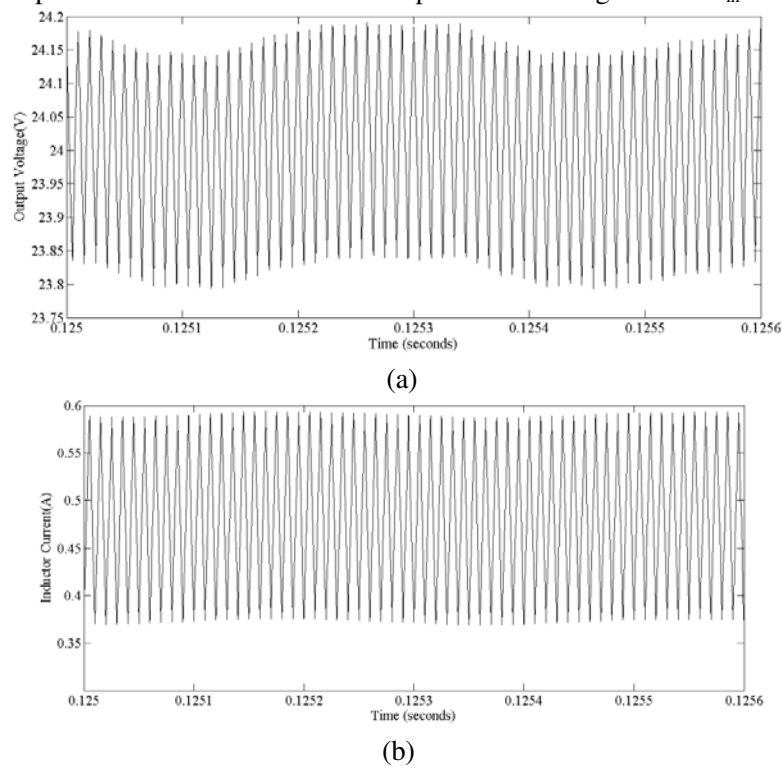
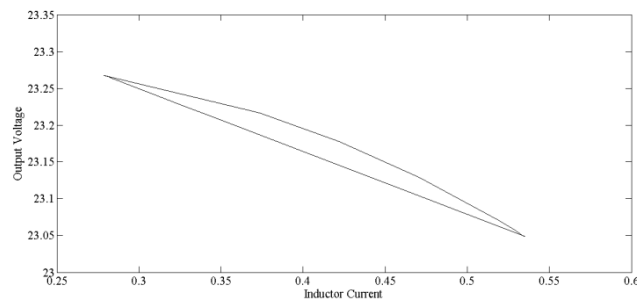


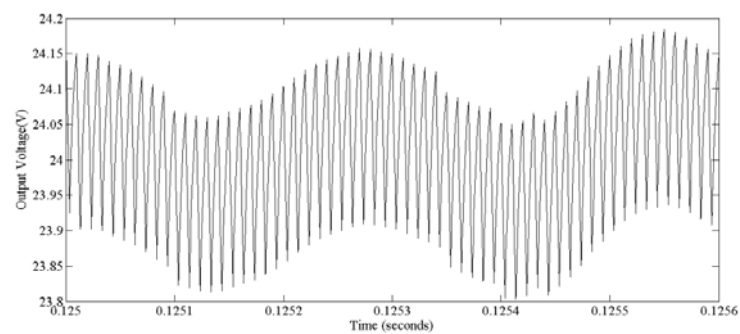
Figure 12. (a) Output voltage waveform (b) Inductor current waveform (c) Phase portrait for Period 4 operation of boost converter after optimization using BFA at $V_{in} = 20$ V



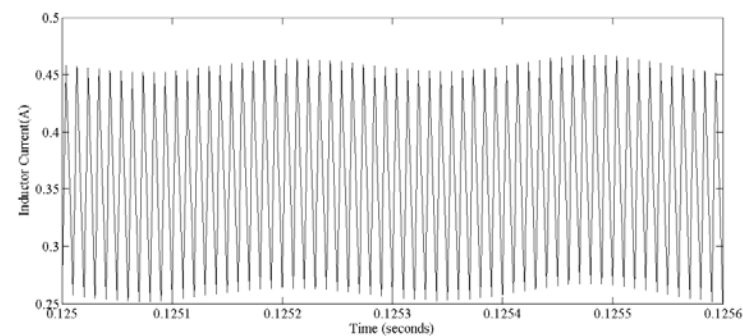


(c)

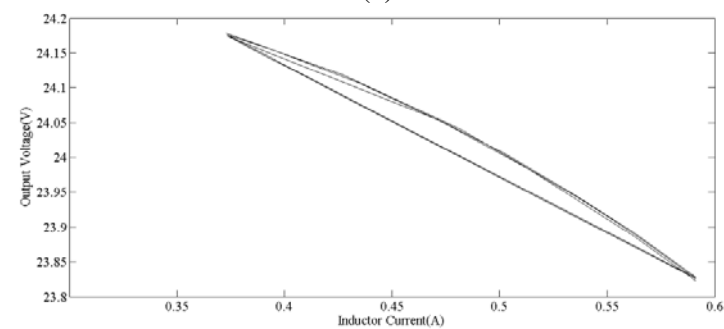
Figure 13. (a) Output voltage waveform (b) Inductor current waveform (c) Phase portrait for Period 1 operation of boost converter after optimization using EBFA at $V_{in} = 12$ V



(a)



(b)



(c)

Figure 14. (a) Outputvoltage waveform (b) Inductor current waveform (c) Phase portrait for Period 1 operation of boost converter after optimization using EBFA at $V_{in} = 16$ V

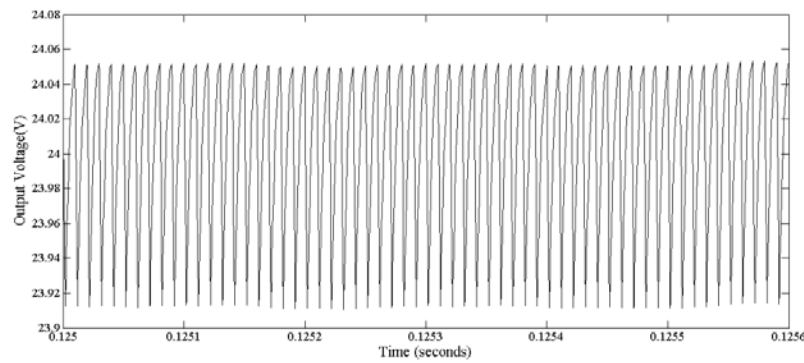


Figure 15. (a)

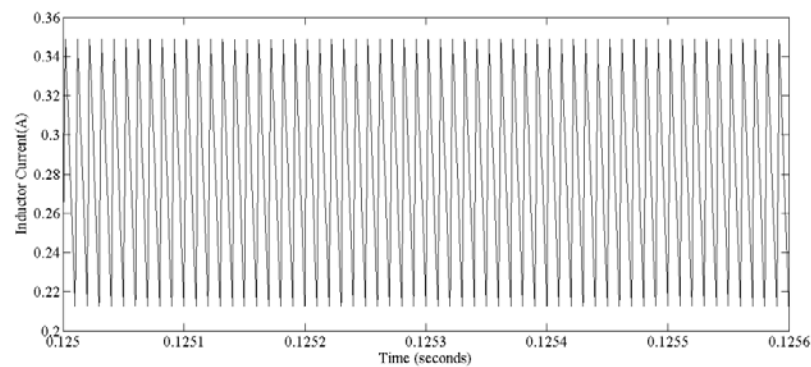


Figure 15. (b)

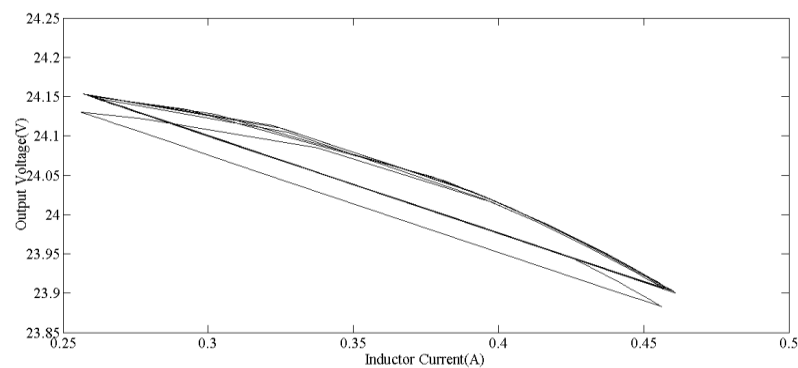


Figure 15. (c)

Figure 15. (a) Outputvoltage waveform (b) Inductor current waveform (c) Phase portrait for Period 2 operation of boost converter after optimization using EBFA at $V_{in} = 20$ V

7. Bifurcation Analysis

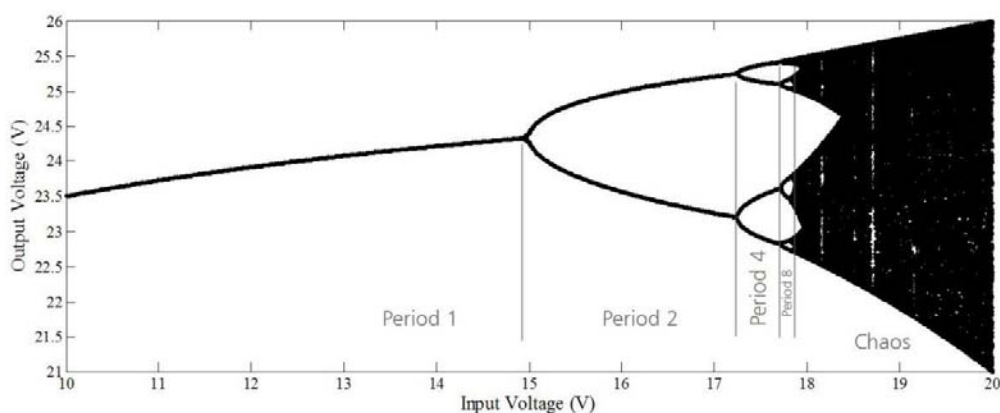
Bifurcation analysis is the appropriate method to describe the undesirable nonlinear behavior of the system. In which, One parameter (in this case V_{in}) is varied while the output voltage is kept unchanged. The

value of this parameter (V_{in}) is plotted along the x-axis and the asymptotic steady-state behavior of one of the discrete state variables is plotted along the y-axis. This bifurcation plot conveys us that the periodic behavior was first transformed to the period-2 sub harmonic, which subsequently led to chaotic regime. Such a qualitative variation in the system behavior is called a bifurcation.

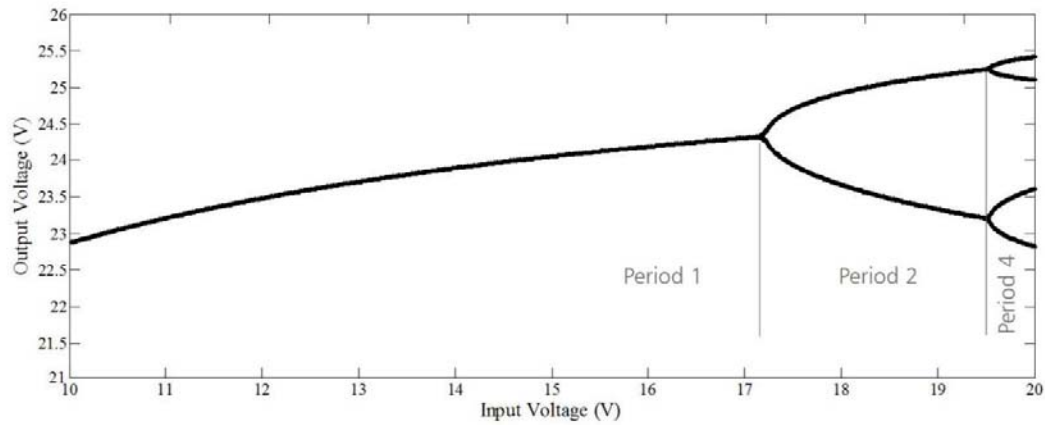
The bifurcation curve of the system before and after optimizing the parameters using BFA and EBFA are shown in Figure.16 (a), Figure. 16 (b) and Figure.16 (c). The bifurcation curve is plotted for output voltage w.r.t input voltage. It is observed that the system exhibits the period doubling bifurcation. The duration in different bifurcation transition is said as period 1, period 2, period 4 and so on till the chaos. The comparison of different voltage range for different periods are shown in Table 3. For instance, it is observed that at $V_{in}=17.2V$, converter operation is in period 4, period 2 and period 1 before optimizing and optimizing using BFA and EBFA respectively.

Table 3. DIFFERENT OPERATING REGION OF BOOST CONVERTER

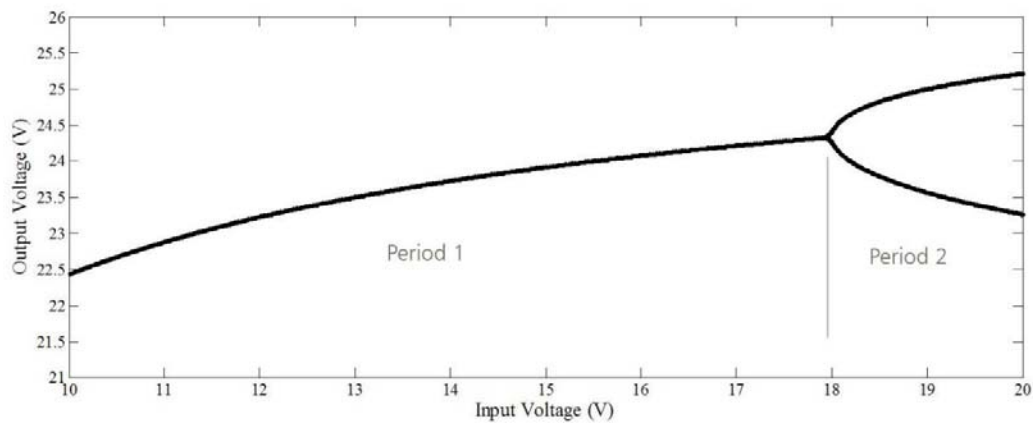
<i>Input voltage range</i>	<i>Boost converter operating region</i>		
	<i>With unoptimized parameters</i>	<i>With BFA optimized parameters</i>	<i>With EBFA optimized parameters</i>
10 V - 14 V	Period 1	Period 1	Period 1
15 V - 17 V	Period 2	Period 1	Period 1
17.2 V - 17.6V	Period 4	Period 2	Period 1
17.7 V - 17.9 V	Period 8	Period 2	Period 1
18V - 20V	Chaos	18V to 19.5V- Period 2 19.6V to 20V- Period 4	Period 2



(a)



(b)



(c)

Figure 16. Bifurcation behavior of boost converter with input voltage (V_{in}) as bifurcation parameter for (a) unoptimized parameters (b) optimized parameters using BFA (c) optimized parameters using EBFA.

The Figure 17. Shows the convergence graph for different techniques. It can be observed that the EBFA takes a bit less number of iteration compared to BFA and it imply that the EBFA takes less computational time than other.

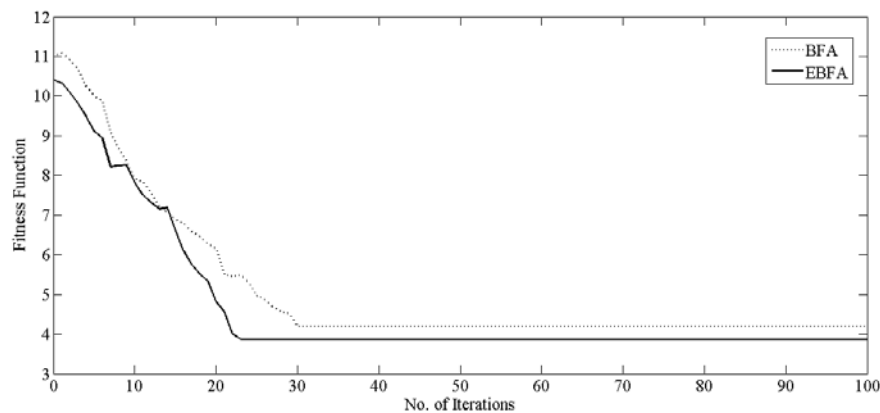


Figure 17. Convergence Graph

8. Conclusion

Controlling of undesirable chaotic behavior in solar fed DC-DC boost converter using optimal parameters is presented in this paper. Well-known Bacterial Foraging Algorithm is enhanced with Nelder-Mead algorithm for optimizing the circuit parameters. The results were obtained using the proposed algorithm and compared with traditional methods. The bifurcation analysis proves that the proposed method is profoundly ensures the stable operation of variable input DC-DC boost converter for the reasonable operating region. This indeed shows the increased range of desirable operating spectrum making it apt for applications involving solar energy. It is inferred that the proposed strategy replaces the complicated design and dedicated auxiliary circuits involved in chaos control for the fast switching DC-DC power converters and thereby the Electro Magnetic Compatibility (EMC) of the converter also improved significantly.

REFERENCES

- [1] Abdullah Abusorrah, Mohammed M Al-Hindawi, Yusuf Al-Turki, Kuntal Mandal, Damian Giaouris, Soumitro Banerjee, Spyros Voutetakis and Simira Papadopoulou 2013 Stability of a boost converter fed from photovoltaic source *Solar Energy* **98** 458-471
- [2] Yumei Zhang, Hong Qin, Yanhua Qu and Jianhua Wu 2012 Chaos Phenomenon in the DC-DC switching converters. *Intelligent Control and Automation (WCICA)* **55(8)** 2039-2043
- [3] P Deiyasundari, R Geetha, G Uma and K Murali 2013. Chaos, Bifurcation and intermittent phenomena in DC-DC converters under resonant parametric perturbation *The European Physical Journal Special Topics* **222(3-4)** 689-697
- [4] J Belwin Edward, N Rajasekar, K Sathiyasekar, N Senthil Nathan and R Sarjila 2013 An Enhanced bacterial Foraging Algorithm approach for optimal Power flow problem including FACTS devices considering system load ability *ISA Transactions* **52 (5)** 622-628
- [5] Tarak Salmi, Mounir Bouzguenda, Adel Gastli and Ahmed Masmoudi 2012 MATLAB/Simulink Based Modelling of Solar Photovoltaic Cell *International Journal of Renewable Energy Research* **2(2)**
- [6] Daniel Hart *Power Electronics* Valparaiso University
- [7] Copeland R Brain 2008 The Design of PID controllers using Ziegler Nichols Tuning
- [8] Quanmin Niu, Zhizhong Ju and Hengli Wang 2009 Study on Bifurcation and chaos in Boost converter based on Energy balance model *Power and Energy Engineering* **1(5)** 27-31
- [9] Woywode O, Weber J, Guldner H, Baranovski A L and Schwarz W 2003 Bifurcation and statistical analysis of DC-DC converters *IEEE Trans. on Circuits and Systems I: Fundamental Theory and*

- Applications* **50(8)** 1072-1080
- [10] K Sundareshwaran and V T Sreedevi 2009 Boost Controller Design Using Queen-Bee-Assisted GA *IEEE Trans. on Industrial Electronics* **56 (3)** 778-783
- [11] Munoz M A, Halgamuge S, Alfonso W and Caicedo E F 2010 Simplifying the Bacteria Foraging Optimization Algorithm *IEEE Congress on Evolutionary Computation (CEC)* **33(8)** 1-7
- [12] L Premalatha and P Vanajaranjan 2008 Control of chaos in nonlinear switching circuits by selection of optimal system parameters using Genetic Algorithm *IEEE Conference on Industrial Technology (ICIT)* 1-6